Design of Materials for Solar-Driven Fuel Production by Metal-Oxide Thermochemical Cycles

by Mark D. Allendorf, James E. Miller, and Anthony H. McDaniel

Although mounting evidence indicates that climate change is anthropogenic,[1-5] demand for energy continues to increase, particularly in developing countries. The U.S. Energy Information Administration predicts in their 2013 outlook that world energy demand will increase 56 percent from 2010 to 2040, driven largely by non-OECD Asia.[6] As seen in Fig. 1, liquid fuels constitute the largest portion of this consumption and are projected to remain so, in spite of expected rising prices. Nearly two thirds of the predicted 38% increase by 2040 in consumption of liquid fossil fuels is due to the transportation sector. This trend will be very difficult to reverse for numerous reasons, including factors such as the structure of cities, relative unavailability of public transportation, reluctance of governments to adopt climate-friendly transportation policies, and historical behavior patterns. Consequently, liquid transportation fuels likely will remain in use for the foreseeable future, particularly since the infrastructure for transporting and delivering liquid fuels to its points of use will be extremely expensive to replace. Development of carbon-neutral routes to liquid fuels is thus a must if the impacts of climate change are to be mitigated and ultimately reversed.

Production of fuel by synthetic means is not a new problem. During World War II, Germany produced hydrocarbon fuels using Fischer-Tropsch chemistry and coal as a carbon source. However, methods of producing carbon-neutral liquid fuels are, for the most part, largely in the realm of research. Even first-generation biofuels (*e.g.* ethanol) are arguably not carbon-neutral.[7] Approaches receiving considerable attention currently include advanced biofuels (*e.g.* algal biodiesel production and cellulosic ethanol),[8] artificial photosynthesis,[9] and solar-driven electrolysis (solar cell + electrolyzer).[10] The latter provides a useful tool for benchmarking new fuel production technologies, since both electrolyzers and solar-electric power are well-understood technologies. Average annual solar-to-fuel efficiencies (AASFE) as high as 18% for production of hydrogen are predicted to be achievable by this approach.[11]

An alternative approach is to use thermochemical cycles that divide the energetically unfavorable thermolysis of water or carbon dioxide (temperatures >3000°C) into two or more reactions that have much more appealing thermodynamics. Many such cycles have been proposed, including hybrid sulfur, sulfur-iodine, zinc oxide, and various other metal oxides. Of these, metal oxides are attractive due to typically low material cost, lack of hazardous or toxic products or intermediates, relative simplicity, and importantly, the potential to achieve high AASFE. A generic two-step metal oxide cycle is as follows:

$$\frac{1}{\delta}MO_X \rightarrow \frac{1}{\delta}MO_{X-\delta} + \frac{1}{2}O_2 \quad \text{at } T = T_{TR}$$

(1; thermal reduction)

$$\frac{1}{\delta}MO_X - \delta + (CO_2 \textit{ or } H_2O)$$
$$\rightarrow \frac{1}{\delta}MO_X + (CO \textit{ or } H_2) \quad \text{at } T = T_{CDS} \text{ or } T_{WS}$$

(2; CO_2 or H_2O splitting)

$$CO_2 \rightarrow CO + \frac{1}{2}O_2 \textit{ or } H_2O \rightarrow H_2 + \frac{1}{2}O_2$$

(3; CO_2 or H_2O thermolysis)

Accounting for thermochemical, collection, and processing efficiencies, solar thermochemical fuel production (STFP) cycles of this type using "non-volatile" metal oxides could achieve AASFE in excess of 25% using a dish solar collector, assuming the development of an advanced working metal oxide substrate.

Guidelines for Material Selection

A large number of diverse metal oxides have been proposed for STFP,[12] including stoichiometric compounds such as ferrites and other transition metal spinels, zinc oxide, Nb_2O_5/NbO_2, CdO/Cd, In_2O_3/In, WO_3/W, SnO_2/Sn, ceria and doped cerias, and most recently, perovskites. Many of these are no longer under consideration for a variety of reasons, including cost, reduction temperature, and conversion efficiency. These oxides fall into two basic categories: non-volatile and volatile. Those within the latter class produce a volatile metal, such as In or Zn, that exists in the gas phase at the required thermal reduction temperature. Volatile oxides are less attractive from a processing point of view because the metal product must be quenched (cooled, condensed, and separated from the O_2 product) to prevent the oxide from reforming via the reverse of reaction 1. Consequently, the most actively investigated materials currently are the non-volatile oxides ferrites and ceria.

It is tempting to conclude that, given this relatively small number of oxides, identifying an "ideal" metal oxide would be relatively straightforward. Unfortunately, such is not the case; a large number of material- and

(continued on next page)

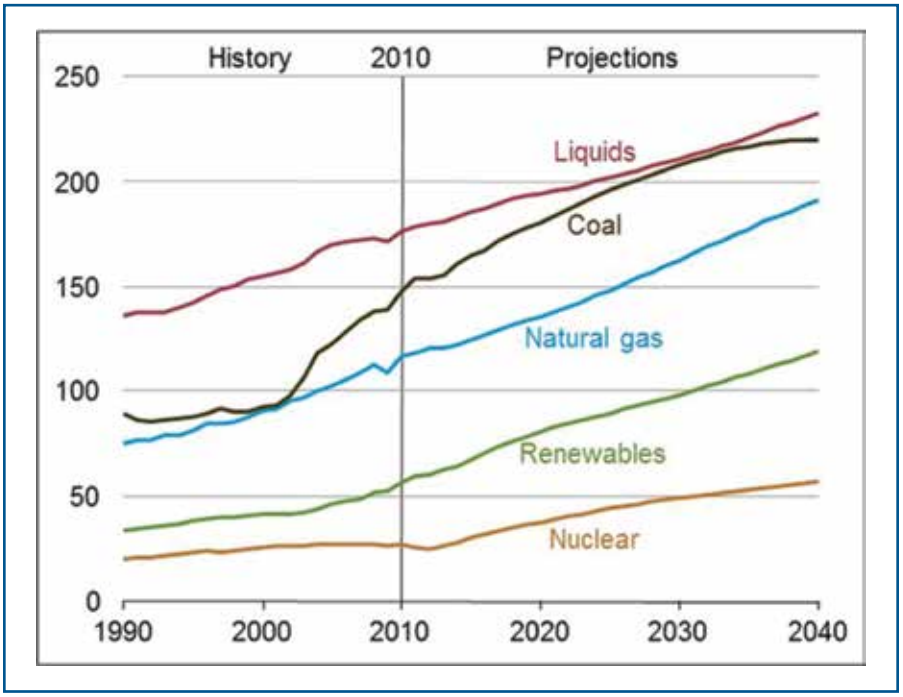

Fig. 1. *World energy demand (in quadrillion Btu) until 2010, with projections to 2040. Data obtained from USEnergyInfoAdmin 2013 Energy Outlook.[6]*

process-specific factors can have a strong effect on the performance of a given metal oxide couple, as shown schematically in Fig. 2. Material-specific properties of concern include reaction thermodynamics, volatility (in spite of the appellation "non-volatile," even a material as refractory as ceria has a finite, and potentially corrosion-inducing, vapor pressure), transport and reaction kinetics, and microstructure. Alternatively, process-specific aspects such as operating temperature, oxygen partial pressure, radiation loss, and reactor materials impact choices for the active metal oxide material and ultimately determine not only the AASFE, but also reactor construction cost and lifetime. In a detailed examination of many of these factors, we concluded that the concept of an ideal material must be considered in the context of the entire process, and not on the basis of, for example, thermodynamics alone.[13]

Fortunately, it is possible to estimate boundaries for material properties based on efficiency and operational targets.[13] The resulting "design guidelines," which are summarized in Table I, simplify the task of identifying an optimal material. Note that the properties listed are both intrinsic (*e.g.*, melting point) and extrinsic (*e.g.*, thickness) characteristics, but also include aspects of process design that are influenced by factors other than the properties of the active material. The rationale for each of these is summarized briefly below; a more detailed discussion is available elsewhere.[13]

Operating temperature window.—This parameter is determined by a set of interacting factors, including reaction thermodynamics, target efficiency, and durability of reactor materials. Nevertheless, thermodynamics and basic engineering considerations allow us to establish approximate upper ($T_{TR} = T_{max}$, Reaction 1) and lower temperature ($T_{GS\ or\ CDS} = T_{min}$, Reaction 2) limits. Almost certainly, T_{TR} will not exceed ~ 1500°C in a practical system due to concerns with materials of construction and challenges in minimizing thermal losses as the temperature is increased. On the oxidation side of the cycle, T_{GS} should ideally be as close to 25°C as possible, to maximize the thermodynamic driving force (possible extent) of the reaction. In this case, however, the kinetics of the gas splitting reaction will almost certainly require higher operating temperatures. The activation energy for reoxidizing zirconia-supported cobalt ferrite using steam, for example, is 141 kJ mol^{-1} and significant H_2 production rates are not observed until temperatures of 900°C are reached.[14] An additional, less obvious, concern is that the greater the temperature swing the greater the amount of sensible heat required to heat the oxide from T_{CDS} to T_{TR}. Coupling this sensible heat load to that needed for heating the carbon dioxide from T_{CDS} or T_{WS} to the reaction temperature, and taking into consideration the effectiveness at which heat can be recuperated within the cycle between T_{TR} and T_{CDS}, the actual gas splitting temperature should be expected to exceed 500°C with an optimal temperature difference during operation (T_{TR}-T_{CDS}) of less than 500°C.

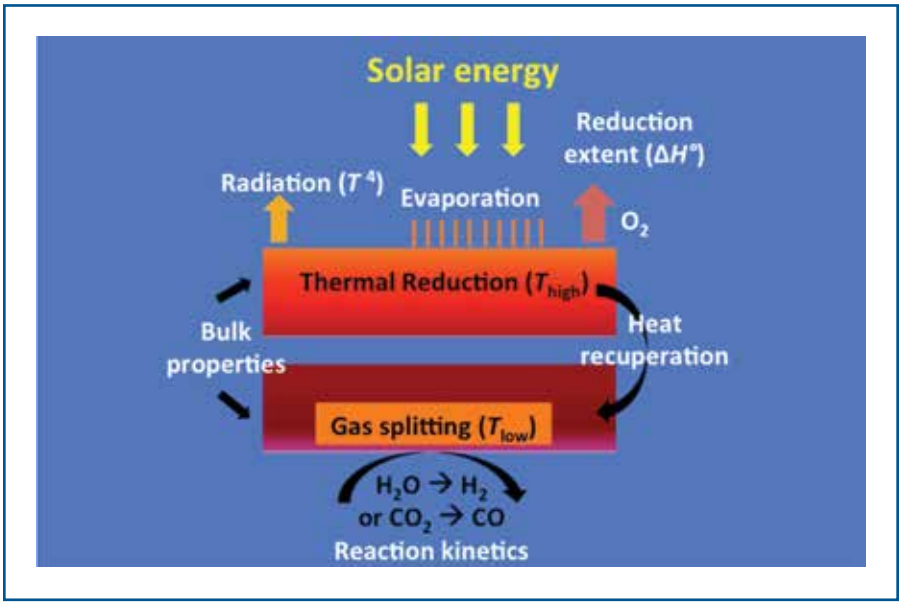

Fig. 2. *Phenomena and material properties that must be considered in developing an optimal material for an STFP cycle.*

Table I. Properties and considerations for an "ideal" STFP working oxide.

Property	Boundary	Comments
Region of thermodynamic favorability	Reduction (R1): 800 ≤ T_{TR} ≤ 1500°C Gas splitting (R2): 25 ≤ T_{GS} ≤ 400°C	Max eff. for T_{TR} = 800 and T_{GS} = 25, (1500, 400) = 72%
Vapor pressure @ T_{TR}	< 2 x 10^{-5} Pa	Langmuir equation estimates loss <0.1 mm/y
Melting Point	> 3275°C	Microstructure stability, unlikely to be met.
Geometry/Structure	Thermal and mass diffusion length ≥ characteristic dimension. Macrostructure scale consistent with thermal stresses in implementation.	Maximize utilization of active material. Avoid breakage and degradation.
Reaction kinetics	Chemical flux matched to solar energy flux.	100% eff ≈ 3.5 μmol CO/s-Watt, T_{GS} > 400°C likely required.

Reaction thermochemistry.—The ideal constraint on the thermodynamics of Reactions 1 and 2 is that both must be spontaneous under operating conditions, *i.e.*, the Gibbs free energy ΔG must be negative within the operating temperature window. To the extent that they are not, additional work, *e.g.* pump work, must be added to the system to drive the reaction. This is an important consideration since the temperature separation between the regions of thermodynamic favorability are likely to be larger than the 500°C suggested above (Table 1). Meredig and Wolverton (MW) developed an analytical framework for assessing the suitability of a given material, reducing the thermodynamics to a form in which only the material-specific properties are considered. These authors illustrated their method using various stoichiometric reactions for known thermochemical cycles (*e.g.*, $Fe_3O_4 \rightarrow 3FeO + 0.5O_2$).[15] Subsequently, we extended their approach to non-stoichiometric materials, such as ceria, doped ceria, and partial reduction of ferrites. Not surprisingly, the range of favorable thermodynamic values is a complex function of operating conditions and the extent of reduction. Both the temperatures of thermal reduction and gas splitting have a strong influence. The O_2 partial pressure during the reduction step is also important; practical considerations (pump work, equipment size, the energy losses and heat loss associated with a diluent gas) suggest that a practical $P(O_2)$ lower limit is 100 Pa. Nevertheless, one can define regions of thermodynamic favorability in which the range of acceptable enthalpy of thermal reduction values is a function of the entropy of reduction. The example data plotted against the MW analysis in Fig. 3 show that complete reduction of $NiFe_2O_4$ to an overall stoichiometry of $NiFe_2O_{3.0}$ is achievable

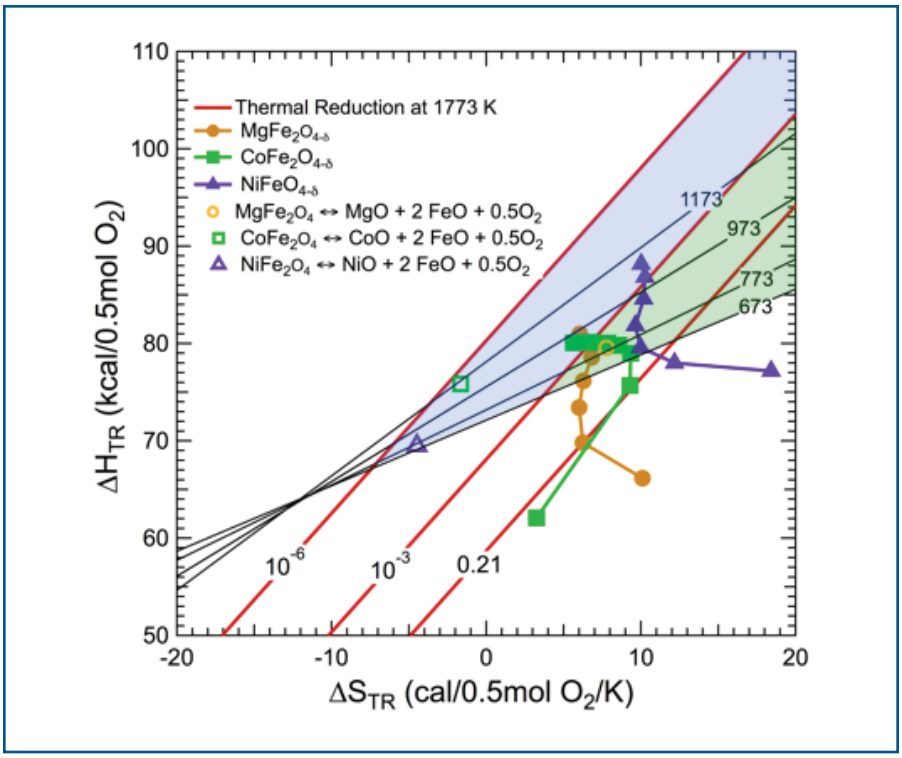

Fig. 3. *Regions of thermodynamic favorability for metal-substituted ferrites, assuming thermal reduction at 1773 K, various O_2 partial pressures during the reduction step, and a range of gas splitting temperatures (shown here for CO_2 splitting). Closed symbols correspond to increasing values of δ in equations 1 and 2. Open symbols correspond to the specific reactions in the legend. See Ref. 13 for additional information*

only if $P(O_2)$ is reduced to 10^{-3} atm (green-shaded region), well below the practical limit. However, within the blue-shaded region ($P(O_2) = 10^{-6}$ atm) these ferrites can be reduced to $NiFe_2O_{3.7}$. In neither case is complete reoxidation feasible; the right-most data point corresponding to $NiFe_2O_{3.99}$ lies outside both the green- and blue-shaded regions.

Vapor pressure of working oxide.—Although many oxides considered for STFP are considered "non-volatile," at the high reaction temperatures required, even materials as refractory as ceria have a non-negligible vapor pressure. Consequently, long exposure to flowing gas can vaporize the material and reduce fuel production capacity or result in downstream contamination-related operational failures. In general, oxides containing transition metals will form diatomic oxides (*e.g.*, FeO, NiO, *etc.*) under thermal reduction conditions and much more volatile metal hydroxides in the presence of water vapor. An estimate of the evaporative loss rate can be obtained from the Langmuir sublimation model, with knowledge of the material's vapor pressure as a function of temperature.[16] This model will likely overpredict the mass loss rate, but nevertheless provides a useful guide and can provide estimates of maximum operating temperatures needed to maintain an acceptable mass loss rate. Losses <0.1 mm/year are predicted if the vapor pressure above the oxide is less than ~ $2x10^{-5}$ Pa. For ferrites, temperatures (T_{TR}) <1270 °C are required to avoid possible mass loss rates greater than 10 mm/year (considered severe in this application). Ceria, in contrast, forms CeO and CeO_2, but due to their much lower vapor pressures the Langmuir model predicts that at temperatures up to 1500°C the vaporization rate is less than ~ 1 mm/yr. The lower temperatures possible for reoxidation using ceria also favor low mass loss rates. These results illustrate how factors beyond the thermochemistry of the reaction must be evaluated to develop effective materials for STFP.

Microstructural stability.—The high temperatures necessary for STFP will also increase mass transport rates, causing sintering of particles and closure of porosity. Previous investigators have seen reductions in capacity and decreased reaction rates for ferrites as a result of rapid mass transport, requiring the use of supports to stabilize the material.[14,17-19] Empirical observations from high-temperature materials science provide guidelines for selecting materials that will be reasonably stable during STFP over many cycles. The Tamman ($0.5T_{mp}$; bulk-to-surface migration) and Hüttig ($0.33T_{mp}$; 2-d mobility, agglomeration on surfaces) temperatures, in conjunction with the melting point (T_{mp}), allow one to assess the microstructural stability. Sintering and creep become significant at ~$0.4T_{mp}$. Based on these criteria, if T_{high} is 1500°C then T_{mp} must be at least 3300°C, a value possessed by very few materials. Some qualitative conclusions can therefore be reached. First, conventional approaches to increase the rates of surface-limited reactions cannot be employed as micro-porosity is unlikely to be maintained. Similarly, stationary packed beds of fine particulates can be expected to eventually sinter and densify into a single solid mass possibly impeding gas transport or leading to other operational difficulties. Therefore, from a durability standpoint, STFP materials are probably limited to larger length scales and/or to systems that account for a regeneration of the physical form.

Reaction kinetics.—The rates of Reactions 1 and 2 are among the least well characterized aspects of thermochemical cycles. In the absence of kinetic data, however, it can be stated that achieving high AASFE requires that energy consumption of the reactions (*i.e.*, endothermic reduction), and hence the reaction rates, be matched to the solar flux entering the system. To the extent that these are not matched, heat must be rejected, which decreases the efficiency. Although the temperatures used are very high, kinetic data we obtained for ferrites and perovskites (see below) show that both Reactions (1 and 2) are thermally activated. The gas splitting step (Reaction 2) is not typically at equilibrium, for example.[14,20] Additional energy to surmount the activation barrier of the reaction is required to drive it at an acceptable rate.

Assessment of Current Materials

Ferrites and other spinels.—Ferrites ($A_xFe_{3-x}O_4$) have received considerable attention because of their favorable thermodynamics, which enable deep reduction. Thermal reduction of ferrites leads to wüstite (Fe_xO in the case of Fe_3O_4 $x \leq 1.0$), a non-ideal solution phase that is hyperstoichiometric in oxygen. The use of Fe_3O_4 for solar fuel production is well studied but not practical because of the relatively low melting point of FeO (liquid-phase products present material handling issues for STFP cycles). However, metal-substituted ferrites, including those with A = Mg, Mn, Co, Ni, and Zn, are more attractive because the wüstite product phase has a higher melting point. Examples of thermodynamic cycles for splitting both CO_2 and water have been reported.[12,13] Thermodynamic analysis predicts that the theoretical efficiency of the reaction step (accounting only for the endotherm of Reaction 1) can exceed 70% for $NiFe_2O_4$ and $CoFe_2O_4$ if the ferrite is thermally reduced to an overall composition of $MFe_2O_{3.5}$ (50% of the maximum, assuming full reduction to wüstite). This requires reducing the O_2 partial pressure to below 100 Pa.[13]

Another material involving a spinel structure is the so-called hercynite cycle, in which a metal-substituted ferrite, such as $CoFe_2O_4$, reacts with Al_2O_3 to form $CoAl_2O_4$ and $FeAl_2O_4$ (hercynite). An advantage of this reaction is that the onset of reduction occurs at 940°C, ~ 150°C lower than other

(continued on next page)

ferrites due to the thermodynamic driving force provided by the formation of alumina. However, the thermodynamics of H_2O + $FeAl_2O_4$ reaction are not as favorable as with FeO; H_2O splitting is not spontaneous, requiring an out-of-equilibrium condition (*e.g.*, a sweep gas) to drive the reaction to products. Both isobaric[21] and isothermal[22] water splitting cycles based on this reaction have been proposed.

Unfortunately, some serious impediments arise with ferrites. First, the relatively low melting point makes sintering fast on the timescale of the reactions, leading to poor cycling behavior. This can be remedied by supporting or solubilizing the ferrite on/into a material such as yttria-stabilized zirconia (YSZ), but this reduces the gravimetric and volumetric capacity. Second, the oxidation reaction involves an initial fast surface-limited phase, but the reaction quickly evolves to one controlled by mass diffusion. This occurs because the ferrite product layer forms a shell around the reduced (wüstite) phase through which oxygen transport is very slow.[14,23] Finally, the wüstite phase is relatively volatile and volatile hydroxides can form in the presence of water vapor (see above). This may be somewhat less of a problem for the hercynite cycle; since the reduction can occur at lower temperatures, volatile iron hydroxides can still form and may limit the durability of this material as well.

Ceria and doped ceria.—Ceria is a non-stoichiometric oxide that loses oxygen at high temperatures by forming vacancies and corresponding Ce^{3+} ions and corresponding Ce3+ ions. Because of its high electron and oxygen ion mobility, it has been considered as an electrode material or the electrolyte in solid oxide fuel cells.[24] Consequently, no phase change occurs, which minimizes potential problems with mechanical stresses for example. This oxide is, however, extremely refractory, having a $P(O_2)$ < 10^{-8} atm at 1300°C, more than five orders of magnitude lower than $NiFe_2O_4$. At the limits of realistic operating conditions, which we consider to be $P(O_2)$ = 100 Pa (10^{-3} atm) and 1500°C thermal reduction temperature, ceria can only be reduced to ~ $CeO_{1.98}$. This realistically limits process efficiencies to values that are too low for practical commercial use; for example, Furler *et al.* recently reported an average efficiency of only 1.73% when operating at ~ 1600°C.[25] Doped cerias initially offered some hope that the reduction temperature could be reduced. Transition-metal dopants are thought to provide the greatest lattice destabilization (and thus, the largest increase in $P(O_2)$), but many lanthanide-doped materials are known as well. Unfortunately, thermodynamic analyses indicate that little or no improvement is to be expected.[13,26] Experimental results are consistent with these predictions. Although all dopants reduce the enthalpy of reduction, this benefit is offset by a concomitant decrease in entropy. Transition-metal dopants also suffer reversibility problems, due either to permanent reduction of their oxidation state or the formation of stable product phases. It is therefore unlikely that either ceria or doped ceria will be of practical use for STFP.

Perovskites.—Recently, a novel class of perovskites (general formula ABO_3) was reported that provides considerably higher H_2 and CO yields than ceria. Based on the hypothesis that a perovskite stable under both the reducing and oxidizing steps of a thermochemical cycle, such as $LaAlO_3$, could be doped with Mn on the B site and Sr on the A site to create a redox-active material that is phase-stable upon oxygen depletion. The resulting material, $Sr_xLa_{1-x}Mn_yAl_{1-y}O_{3-\delta}$, produces up to nine-fold higher H_2 and six-fold higher CO yield when reduced at 1350°C and reoxidized at 1000°C (Fig. 4).[20] Oxygen evolution begins 300°C lower than undoped ceria and at comparable reaction rates (see discussion below). Cycling experiments indicate that this capacity is maintained over at least 80 cycles, a considerable improvement over metal-substituted ferrites. Conceivably, perovskite compositions with even better performance may exist, but discovering these is complicated by the large composition space that can adopt the perovskite structure. Notably, a related perovskite, (La, Sr) $MnO_{3-\delta}$, recently investigated by Scheffe *et al.*, can also be used for STFP. Somewhat lower, but still favorable, reduction extents relative to ceria were obtained.[27]

Measurement of Gas-splitting Kinetics

Rates of thermal reduction and gas splitting are largely unknown for the conditions relevant to STFP. Recently, we developed a unique, optically-accessible stagnation flow reactor (SFR) (Fig. 5) that enables these rates to be measured under realistic STFP conditions. This instrument is equipped with a 500 W continuous-wave NIR diode laser for sample heating enabling rapid screening of reaction rates across a range of temperatures and pressures encountered during STFP operation (such as high heating rates (> 100°C/s) at solar concentrations equivalent to 5000 suns). Gas compositions exiting the SFR are measured by mass spectrometry. An important attribute that distinguishes the fluid dynamics of the SFR from flow tube reactors, packed bed reactors, or thermogravimetric analyzers (TGA), which are commonly used to measure kinetic data, is that the gas-phase region above the sample is an ideal 1-D flow field governed by diffusive transport. This creates a well-controlled environment for characterizing kinetic behavior.

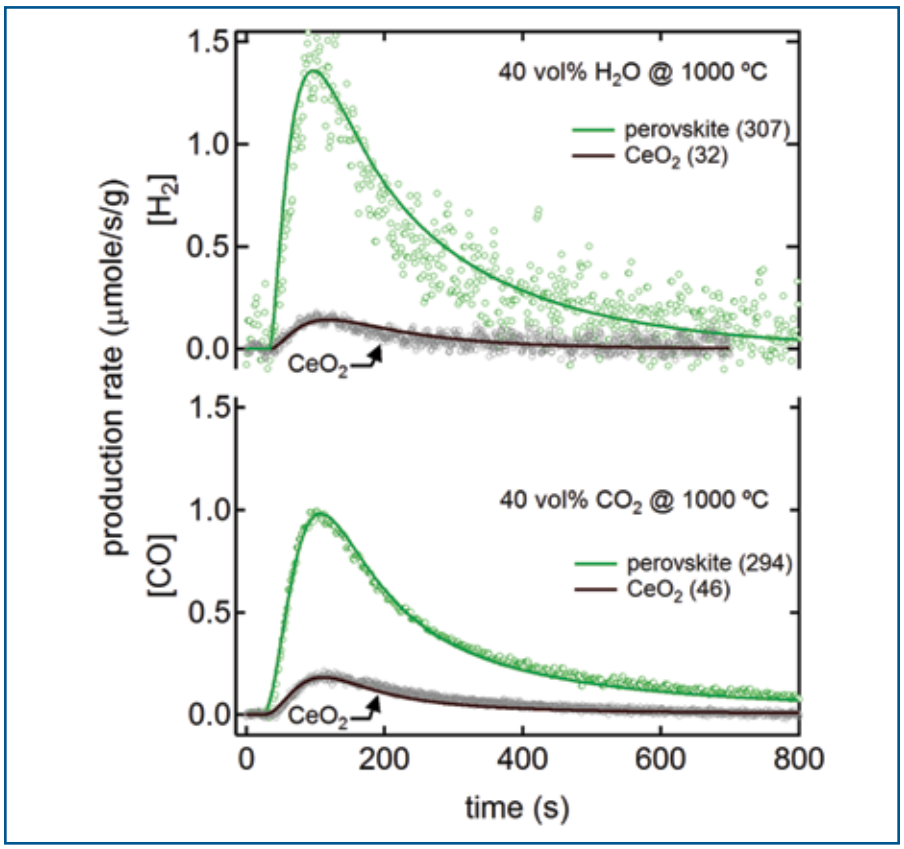

Fig. 4. *H_2 (top) and CO (bottom) production rates as a function of time for a Sr- and Mn-doped $LaAlO_3$, measured during oxidation in 40 vol% H_2O or CO_2 at 1000 °C (green open symbols), compared to CeO_2 (gray open symbols). STFP materials were thermally reduced at 1350 °C in He. The total amount of H_2 or CO produced in mmoles per g material is shown in parentheses. Solid lines are the results of kinetic modeling.*

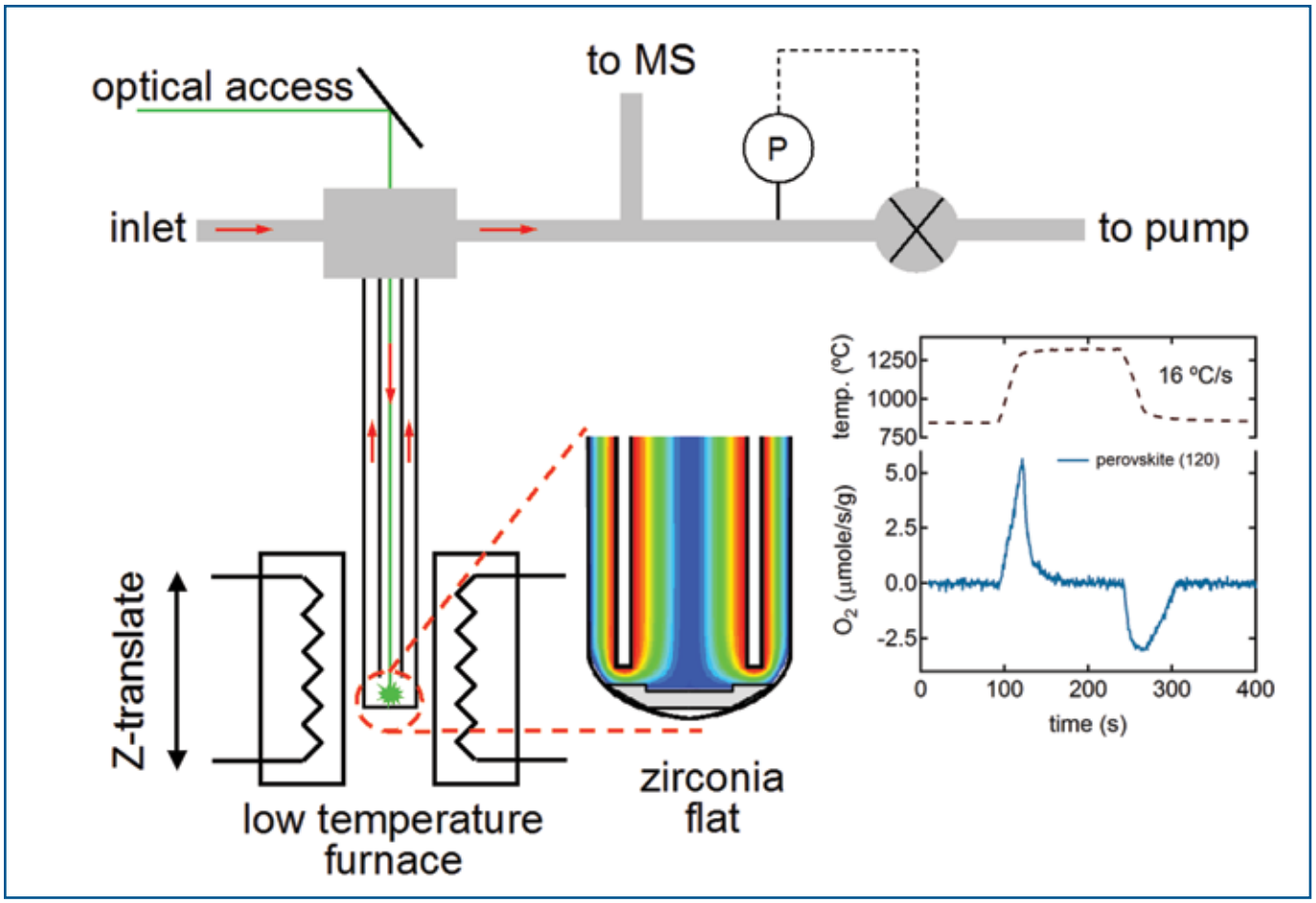

Fig. 5. *Schematic of the Sandia laser-heated SFR. Graph inset shows O_2 uptake and release for a perovskite oxide in a constant background pressure of O_2 heated and cooled at 16°C/s.*

The inset to Fig. 5 illustrates how this approach has been used to resolve the O_2 uptake and release kinetics of a perovskite oxide. In this case, the sample is exposed to a constant partial pressure of O_2 during heating and cooling. As the material heats up, O_2 is liberated from the solid until a new equilibrium is established at the higher temperature (positive O_2 production rate in figure inset). Upon cooling, the solid reabsorbs O_2 from the ambient, which is shown as a negative production rate in the graph. The area under the uptake and release curves measures redox capacity, while the temporal characteristics contain rate information and mechanistic insight. We employed the SFR to measure the kinetics of gas splitting for CeO_2, Sr- and Mn-doped $LaAlO_3$, and mixed metal ferrite-zirconia composite materials.

As mentioned previously, the redox kinetics largely determine the reaction extents and efficiencies that may be realized in practice, and are an important consideration in the reactor design. This is because the AASFE will suffer if the reaction rates are not well-matched to the solar flux. To the extent they are not, then the slower process will hinder reactor throughput unless a mitigating strategy, such as decoupling the residence times in each reaction zone, is used to balance the production of O_2 and CO (or H_2). This tradeoff demonstrates the importance of considering reactor design and material chemistry within the context of redox kinetics.

Topics for Future Research

It is clear that the properties of the active material, including not only the thermodynamics, but also the reactivity, microstructural stability, and volatility, must be understood to develop efficient and economical STFP processes. There is considerable need for additional research concerning all of these properties. In general, there is a broad palette of potential materials of interest that have not been studied at the temperatures required for thermal reduction, creating a major gap in the understanding of their behavior under processing conditions. Future work to develop accurate thermodynamic models, determine reaction kinetics, and predict the evolution of material properties during high-temperature cycling will therefore be essential. Given the large composition space of materials of interest, computational screening will be an invaluable tool, as will high-throughput, automated, synthesis and characterization. Despite these challenges, the scientific and engineering data now available are highly encouraging that STFP can be a viable technology for producing carbon-neutral transportation fuels.

Acknowledgments

This work was supported by the U.S. Department of Energy Fuel Cell Technologies Program as part of the production technology development area and by the Laboratory Directed Research and Development Program at Sandia National Laboratories. Sandia is a multiprogram laboratory operated by Sandia Corporation, a Lockheed Martin Company, for the United States Department of Energy's National Nuclear Security Administration under Contract DE-AC04-94AL85000.

About the Authors

Mark D. Allendorf is a Senior Scientist at Sandia National Laboratories and holds a PhD in inorganic chemistry from Stanford University. He leads efforts to develop novel material solutions to energy- and national security-related problems, involving both fundamental science and applications development. In addition to his work in high-temperature chemistry, he conducts

(continued on next page)

interdisciplinary research to develop metal-organic frameworks for applications such as chemical sensing, radiation detection, hydrogen storage, gas separations, and charge transfer. He is President Emeritus and Fellow of The Electrochemical Society and has won multiple Sandia awards for leadership and teamwork. His research involves postdoctoral fellows, students, and Sandia technical staff members and has more than 140 publications. He may be reached at mdallen@sandia.gov.

James E. Miller has been involved in catalysis and chemical processing research at Sandia National Laboratories for over 20 years, most recently serving as the principal investigator of the laboratories' Sunshine to Petrol (S2P) effort. The goal of S2P is the efficient and cost effective production of hydrocarbon fuels from sunlight, carbon dioxide, and water via chemical means. Dr. Miller has been involved in all multiple aspects of the project including prototype design development and demonstration, materials development, and systems studies. He holds degrees in chemical engineering from Texas A&M University (BS) and the University of Texas at Austin (PhD). He may be reached at jemille@sandia.gov.

Anthony McDaniel is a member of the technical staff at Sandia National Laboratories and holds degrees in chemical engineering from the University of Colorado (Boulder, BSc) and the University of California (Los Angeles, PhD). His current research is focused on thermochemistry and electrochemistry of materials critical to developing sustainable energy technologies. These include complex oxides used in water and carbon dioxide splitting, solid oxide fuel cells, lithium ion batteries, and super ionic conductors. He also leads a program funded by the Department of Energy to develop a solar-thermochemical reactor for the efficient production of hydrogen from concentrated sunlight. He may be reached at amcdani@sandia.gov.

References

1. L. Comte, L. Buisson, M. Daufresne, and G. Grenouillet, *Freshwater Biology,* **58**, 625 (2013).
2. M. Forsius, S. Anttila, L. Arvola, I. Bergstrom, H. Hakola, H. I. Heikkinen, J. Helenius, M. Hyvarinen, K. Jylha, J. Karjalainen, T. Keskinen, K. Laine, E. Nikinmaa, P. Peltonen-Sainio, K. Rankinen, M. Reinikainen, H. Setala, and J. Vuorenmaa, *Current Opinion in Environmental Sustainability,* **5**, 26 (2013).
3. S. Jenouvrier, *Global Change Biology,* **19**, 2036 (2013).
4. M. Koch, G. Bowes, C. Ross, and X. H. Zhang, *Global Change Biology,* **19**, 103 (2013).
5. C. Rosenzweig and P. Neofotis, *Wiley Interdisciplinary Reviews-Climate Change,* **4**, 121 (2013).
6. *International Energy Outlook 2013*; U.S. Energy Information Administration (2013).
7. T. D. Searchinger, S. P. Hamburg, J. Melillo, W. Chameides, P. Havlik, D. M. Kammen, G. E. Likens, R. N. Lubowski, M. Obersteiner, M. Oppenheimer, G. P. Robertson, W. H. Schlesinger, and G. D. Tilman, *Science,* **326**, 527 (2009).
8. V. Menon and M. Rao, *Progress in Energy and Combustion Science*, **38**, 522 (2012).
9. N. S. Lewis, *Interface*, ***22***, 41 (2013).
10. J. Ivy, National Renewable Energy Laboratory Report NREL/MP (2004).
11. N. P. Siegel, J. E. Miller, I. Ermanoski, R. B. Diver, and E. B. Stechel, *Industrial & Engineering Chemistry Research*, **52**, 3276 (2013).
12. T. Kodama and N. Gokon, *Chem. Rev.*, **107**, 4048 (2007).
13. J. E. Miller, A. H. McDaniel, and M. D. Allendorf, *Adv. Energy Mater.,* DOI: 10.1002/aenm.20130046.
14. J. R. Scheffe, A. H. McDaniel, M. D. Allendorf, and A. W. Weimer, *Energy & Environmental Science*, **6**, 963 (2013).
15. B. Meredig and C. Wolverton, C. *Phys. Rev. B*, *80,* 245119 (2009).
16. Lafferty, J. M. *Scientific Foundations of Vacuum Technique*; 2nd ed.; Wiley: New York, 1962.
17. N. Gokon, T. Minno, Y. Nakamuro, and T. Kodama, *J. Sol. Energy Eng.-Trans. ASME*, **130**, 011018, (2008).
18. T. Kodama, N. Gokon, and R. Yamamoto, *Sol. Energy*, **82**, 73 (2008).
19. J. R. Scheffe, M. D. Allendorf, E. N. Coker, B. W. Jacobs, A. H. McDaniel, and A. W. Weimer, *Chem. Mater.*, **23**, 2030 (2011).
20. A. H. McDaniel, E. C. Miller, D. Arifin, A. Ambrosini, E. N. Coker, R. O'Hayre, W. C. Chueh, and J. H. Tong, *Energy & Environmental Science*, **6**, 2424 (2013).
21. J. R. Scheffe, J. H. Li, and A. W. Weimer, *Int'l. J. Hydrogen Energy*, **35**, 3333 (2010).
22. C. L. Muhich, B. W. Evanko, K. C. Weston, P. Lichty,X. Liang, J. Martinek, C. B. Musgrave, and A. W. Weime, *Science*, **341**, 540 (2013).
23. E. N. Coker, J. A. Ohlhausen, A. Ambrosini, and J. E. Miller, *J. Mater. Chem.,* **22**, 6726 (2012).
24. M. Mogensen, N. M. Sammes, and G. A. Tompsett, *Solid State Ionics*, **129**, 63 (2000).
25. P. Furler, J. R. Scheffe, and A. Steinfeld, *Energy Environ. Sci.*, **5**, 6098 (2012).
26. J. R. Scheffe and A. Steinfeld, *Energy Fuels*, **26**, 1928 (2012).
27. J. R. Scheffe, D. Weibel, and A. Steinfeld, *Energy Fuels*, **27**, 4250 (2013).